Korean J. Chem. Eng., **18**(5), 711-718 (2001)

Determination of Decomposition Rate Constants of Volatile Organic Compounds and Nitric Oxide in a Pulsed Corona Discharge Reactor

Young Sun Mok†, Ho Won Lee, Young Jin Hyun, Sung Won Ham* and In-Sik Nam**

Department of Chemical Engineering, Cheju National University, Ara, Cheju 690-756, Korea
*Department of Chemical Engineering, Kyungil University, Hayang, Kyungbuk 712-701, Korea
**Department of Chemical Engineering, Pohang University of Science & Technology, Kyungbuk 790-784, Korea
(*Received 14 June 2001 • accepted 13 July 2001*)

Abstract−The decomposition of toluene, propylene and nitric oxide by using a pulsed corona discharge process was investigated. The performance equation of the pulsed corona reactor was derived with the assumption that the decomposition reaction rate is directly proportional to the concentration of the pollutant and the discharge power. From this model equation and the experimental data, the apparent decomposition rate constants of various gaseous organic compounds and nitric oxide were determined. Alkene and substituted alkene were found to have much larger decomposition rate constants than aromatic compounds and substituted alkane, which indicates that the derivatives of aromatics and alkane cannot readily be decomposed in this system. To verify the validity of the model derived, the experimental data in the present study and in the literature were compared with the calculation results using the decomposition rate constants. Despite the different reactor geometry and experimental condition, good agreement between the experimental data and the calculation results was shown.

Key words: Pulsed Corona Discharge, Volatile Organic Compounds, Decomposition, Rate Constant

INTRODUCTION

Volatile organic compounds (VOCs) and nitrogen oxides (NO_x) emitted from a variety of industrial processes are the main causes of many environmental problems such as photochemical smog, acid rain and ozone depletion. Many researchers have reported that non-thermal plasma or catalyst-hybrid plasma process can be an effective approach to induce chemical reactions for their removal [Choi et al., 2000; Futamura et al., 1998; Oda et al., 1998; Ogata et al., 1999; Snyder and Anderson, 1998; Song et al., 2000]. The pulsed corona discharge process (PCDP) is a common method to create a non-thermal plasma in which electrical energy is used to produce electrons with a high average kinetic energy in the range of 5-10 eV [Jeong et al., 2001; Lowke and Morrow, 1995; Mizuno et al., 1995; Mok et al., 2001; Roush et al., 1996]. The pulse corona discharge develops by forming a number of streamers, the starting points of which are discrete and distributed over the surface of discharging wire. The streamer propagates very fast from discharging wire to grounded plate [Civitano, 1993; Dinelli et al., 1990]. During the propagation, energetic electrons and various radicals are generated, which results in the removal of the air pollutants such as VOCs and NO_x.

According to the literature, much on the removal of VOCs and NO_x using non-thermal plasma has been carried out so far [Lowke and Morrow, 1995; Roush et al., 1996; Shimizu et al., 1997; Song et al., 2000; Tas et al., 1997; Urashima, 1998; van Veldhuizen, 1998]. Especially, the removal of NO_x has widely been studied both experimentally and theoretically. Therefore, the kinetics and mechanisms of the NO_x removal are well known on the whole, and several kinetic models have been proposed [Mok et al., 1998; Sun et al., 1996]. On the other hand, the reaction kinetics and mechanisms of VOC decomposition has been a leaner subject, although many experimental data in terms of removal efficiency and byproducts are available [Futamura et al., 1998, 1999; Krasnoperov, 1997; Ogata et al., 1999; Penetrante et al., 1996; Snyder and Anderson, 1998; Yamamoto et al., 1993].

There are several tens of VOCs including alkanes, alkenes, alcohols, ketones, aromatics, aldehydes, etc. Due to such diverse kinds of VOCs, the determination of the kinetics and mechanisms for all of the VOCs is not easy, and requires much time and effort. In the decomposition of propylene alone, for example, at least more than ten elementary reactions are involved and the rate constant of each elementary reaction is mostly still unknown [Atkinson et al., 1992; Mok et al., 2000; Seinfeld, 1975]. Reaction scheme of more complicated compounds may be more complex and accompany much more elementary reactions. One method to simplify this problem is to express the decomposition with respect to overall reaction. Several researchers assumed that the decomposition is first order reaction in terms of the VOC concentration [Choi et al., 2000; Krasnoperov, 1997]. Although it may partly be true at a fixed discharge power, such assumption makes error at different discharge power because the decomposition rate is also dependent on the concentrations of the active species such as energetic electrons, radicals, ions, etc. As clarified in the previous studies, the concentrations of the active species are proportional to the discharge power [Mok et al., 1998; Penetrante et al., 1996; Sun et al., 1996]. Therefore, the decomposition rate should be expressed in terms of both the concentration and the discharge power, which makes it possible to obtain more useful decomposition rate constants from the practical point

†To whom correspondence should be addressed.
E-mail: smokie@cheju.cheju.ac.kr

of view.

In this study, the decomposition of VOCs and the removal of nitric oxide by the pulsed corona discharge were investigated. A plug flow model equation expressing the performance of the corona reactor was derived by using the simplified reaction mechanism, and the apparent decomposition rate constants of various organic compounds and nitric oxide were determined. Propylene, toluene and nitric oxide were chosen as the pollutants for the experiments, however, the decomposition rate constants of the other VOCs were also determined by using the extensive experimental data in the literature [Krasnoperov, 1997; Penetrante et al., 1996; Roush et al., 1996; Snyder and Anderson, 1998; Song et al., 2000]. In order to verify the validity of this study, the experimental data were compared with the calculation results.

REACTOR MODEL

At steady state the material balance of a component over reactor length can be expressed as follows:

$$D_e\frac{dC_A^2}{dz^2}-u_0\frac{dC_A}{dz}-R_A=0 \tag{1}$$

where D_e is the axial dispersion coefficient, C_A is the concentration of the pollutant at any position, u_0 is the linear velocity, z is any position, R_A is the decomposition rate of the pollutant.

In most cases of gas flow system, the axial dispersion can be neglected because no mixing process is involved and there is nothing to disturb the flow axially. In addition, the radial uniformity of the concentration can be assumed because the propagation velocity of the streamer from the discharging wire to the cathode is very fast [Civitano, 1993], and then, Eq. (1) can be abbreviated as

$$-u_0\frac{dC_A}{dz}=R_A \tag{2}$$

If the time taken to move the distance z at a linear velocity u_0 is defined as τ, Eq. (2) is equated as

$$-\frac{dC_A}{d\tau}=R_A \tag{3}$$

When the total residence time of the gas stream (reactor length/linear velocity or reactor volume/gas flow rate) is τ_L and the pulse repetition rate is f, the total number of pulses accepted by the gas stream during passing through the reactor is equal to $f\tau_L$, i.e., the gas stream is processed by $f\tau_L$ pulses. The time that each pulsing can treat the gas stream is equivalent to the pulse period (τ_P) given by

$$\tau_P=\frac{1}{f} \tag{4}$$

The decomposition rate of VOC depends on both the concentration of itself and the concentrations of the active species generated in the corona reactor. Note that the concentrations of the active species generated are proportional to the discharge power applied to the reactor volume. Therefore, the decomposition rate can be written as follows:

$$R_A=k_dC_AP_W/V_R \tag{5}$$

where k_d is the decomposition rate constant, V_R is the reactor volume and P_W is the average discharge power expressed as

$$P_W=fE_P \tag{6}$$

where E_P is the energy delivered to the corona reactor per pulse.

Substitution of Eq. (5) for Eq. (3) gives

$$-\frac{dC_A}{d\tau}=k_dC_AP_W/V_R \qquad (\tau=0\sim\tau_P) \tag{7}$$

Since the only dependent variable in Eq. (7) is C_A, it can easily be integrated to give

$$\ln\frac{C_{A,i-1}}{C_{A,i}}=k_d\tau_PP_W/V_R \qquad (i=1, 2, 3, \ldots f\tau_L-1, f\tau_L) \tag{8}$$

where $C_{A,i-1}$ and $C_{A,i}$ are the concentrations of the volatile organic compound before and after treated by i-th pulsing.

Since the total number of pulses accepted by the gas stream is $f\tau_L$, Eq. (8) should be extended from i=1 to i=$f\tau_L$ in order to obtain the concentration at the reactor outlet. Thus, the performance equation for this system becomes

$$\ln\frac{C_{A0}}{C_{AL}}=\sum_1^{f\tau_L}k_d\tau_P=\frac{P_W}{V_R}=k_d\tau_P\frac{P_W}{V_R}f\tau_L \tag{9}$$

Eq. (9) can be simplified as below since the pulse period (τ_P) is the reciprocal of the pulse repetition rate (f):

$$\ln\frac{C_{A0}}{C_{AL}}=k_d\tau_LP_W/V_R \tag{10}$$

Rearranging Eq. (10) with respect to the decomposition rate constant,

$$k_d=\frac{V_R}{\tau_LP_W}\ln\frac{C_{A0}}{C_{AL}} \tag{11}$$

Eq. (11) may be used for the determination of the decomposition rate constant if the concentration at the reactor outlet is measured.

Since the total residence time of the gas stream is equal to the reactor volume divided by the gas flow rate, Eq. (11) can be rewritten as an equivalent form below

$$k_d=\frac{1}{P_W/Q}\ln\frac{C_{A0}}{C_{AL}} \tag{12}$$

In Eq. (12), P_W/Q indicates the energy density (or specific energy), and it has widely been used as a key parameter in this field of nonthermal plasma discharge process.

EXPERIMENTAL

Fig. 1 depicts the schematic of the corona discharge reactor that consists of stainless steel wires and plates. The diameter of the discharging wire is 0.8 mm, and the length and the breadth of each plate are 81 cm and 9 cm, respectively. The distance between the two plates at the top and the bottom is 3 cm, and a number of wires are placed at regular intervals of 1.5 cm between the two plates. The wires are 1.5 cm apart from the plate, and electrically connected one another. The high voltage pulse is applied to the wire, and the plate is grounded. Therefore, the wire and the plate act as the anode

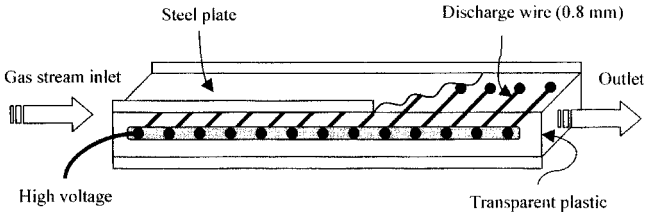

Fig. 1. Schematic description of the pulsed corona reactor.

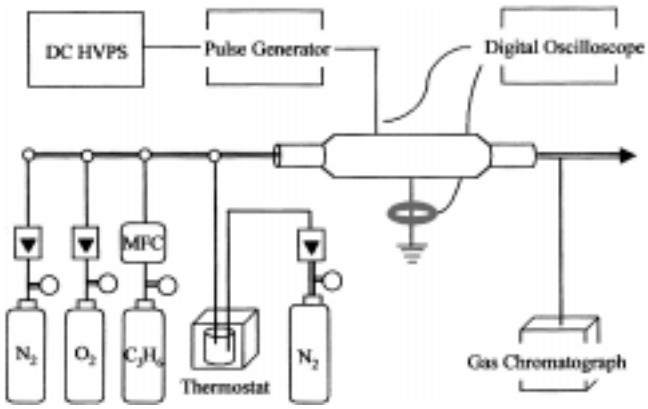

Fig. 2. Schematic of the experimental apparatus.

and the cathode, respectively.

Fig. 2 shows the schematic of the experimental apparatus for the removal of VOCs and NO. Nitrogen and oxygen were used as the background gas, and propylene and toluene were used as the organic compounds. Feed gas stream composed of 80% (v/v) N_2, 20% (v/v) O_2 and the pollutants was directed to the corona reactor. The flow rates of N_2 and O_2 were adjusted by flow meters with the total flow rate kept unchanged, and the flow rates of pure propylene and nitric oxide [premixed NO 10.0% (v/v) in N_2] were controlled by mass flow controllers (Model 1179, MKS Instruments, Inc.). The concentration of toluene was regulated by using its vapor pressure (1.333 kPa at 6.4 °C) as follows. A mass flask containing toluene was immersed in a refrigerating circulator kept at a constant temperature of 6.4 °C. Nitrogen gas whose flow rate was adjusted by a mass flow controller (Model 1179, MKS Instruments, Inc.) was saturated with toluene as it passed through the flask. When N_2 gas is saturated with toluene at this temperature, the concentration corresponds to 13,000 ppm (parts per million volumetric). In this situation, the concentration of toluene in the mixed gas stream can be calculated as

$$C_{TOL}(\text{ppm}) = \frac{1.333}{101.325}\frac{Q_3}{Q_1+Q_2+Q_3}\times 10^6 \quad (13)$$

where C_{TOL} is the desired toluene concentration, Q_1 and Q_2 are the flow rates of N_2 and O_2, and Q_3 is the flow rate of N_2 used for the saturation of toluene. The total flow rate of the mixed gas was changed in the range of 0.033-0.333 L/s.

The removal efficiencies of propylene, toluene and nitric oxide were measured by analyzing the concentration differences at the reactor outlet before and after corona discharge. The concentration of NO was analyzed by a chemiluminescence NO-NO_2-NO_x analyzer (Model 42H, Thermo Environmental Instrument Inc.), and the concentrations of propylene and toluene were analyzed by a gas chromatograph (Hewlett Packard 5890). Byproducts generated as a result of decomposition were identified by a gas chromatograph-mass spectrometer (Platform II, Micromass UK, Ltd.) and a DB-5 capillary column (50 m×0.2 mm×0.33 μm) of J&W Scientific. The concentrations of the identified components were measured by a gas chromatograph equipped with flame ionization detector (FID) and thermal conductivity detector (TCD).

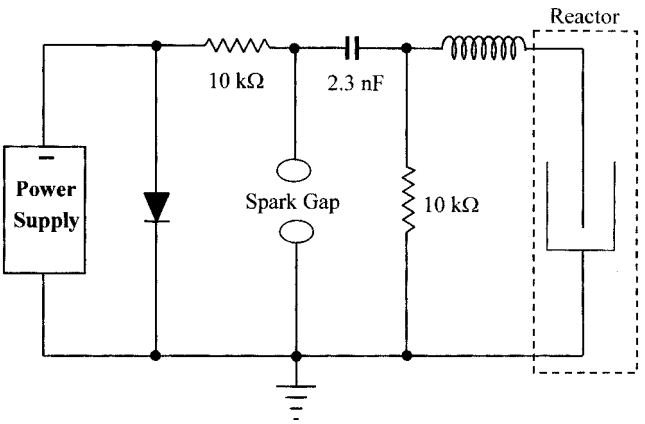

Fig. 3. Schematic of the pulse generation circuit.

The schematic of the high voltage pulse generator is presented in Fig. 3 The pulse-forming capacitor (2.3 nF) is charged by a negative dc high voltage power supply (Glassmann High Voltage Inc.). As the voltage on the capacitor reaches the spark-over voltage of the spark gap electrode acting as a switch, the charge stored in the capacitor flows through a stray inductance to charge the reactor electrode structure. When the voltage between the discharging wire and the grounded plate reaches the corona onset value, corona discharge occurs from the discharging wires. Peak voltage of about 22.7 kV was typically applied to the discharging wire at repetition rate from 10 to 50 Hz (pulses s^{-1}). The pulse repetition rate was varied by adjusting the charging time of the pulse-forming capacitor. For the voltage measurement, a high voltage probe (Tektronix P6015) having DC attenuation of 1000 : 1±3% was used with a digital oscilloscope (Tektronix TDS 620B) of which bandwidth and sample rate are 500 MHz and 2.5 GS/s. For current measurement, a current transformer (Tektronix CT-4), a current probe (Tektronix A6302) and a current amplifier (Tektronix AM503B) were used. The A6302 current probe covers frequencies up to 50 MHz. The CT-4 is a high current transformer that extends the measurement capability of the current probe. The current probe was connected to the current amplifier, which amplifies the current sensed by the current probe and converts the current to a proportional voltage that is displayed on the oscilloscope. The pulse energy delivered to the corona reactor per pulse was calculated with the voltage and current waveforms measured:

$$E_P = \int_0^t VI\,dt' \quad (14)$$

where V is the pulse voltage, I is the pulse current, and t is the pulse width.

RESULTS AND DISCUSSION

1. Voltage and Current Waveforms

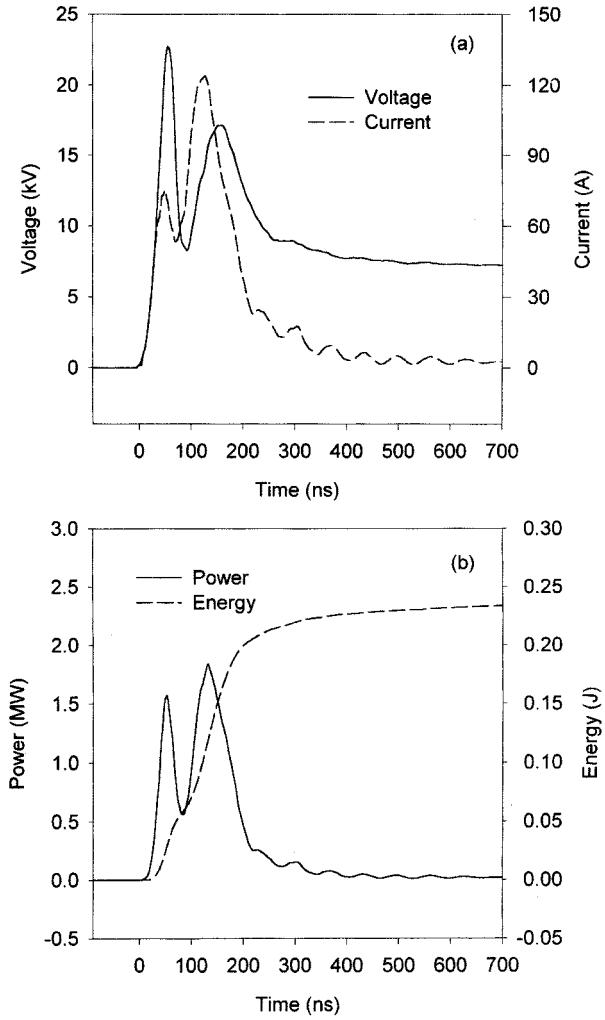

Fig. 4. Waveforms of pulse voltage and current (a), power and energy (b).

Fig. 4(a) shows the voltage and current waveforms measured at the discharging wire and the grounded electrode. When the pulse voltage is applied to the discharging wire, capacitive current flows before the corona onset. When the voltage exceeds the corona onset value, streamer corona develops and the voltage drop is observed. The peak voltage was about 22.7 kV with rise rate of 0.54 kV ns^{-1}, and the pulse width (full width at half maximum) was about 180 ns. The peak current was 124 A, and the pulse current was extinguished at about 300 ns. As presented in Fig. 4(b), the energy delivered to the reactor per pulse was found to be 220 mJ by integrating the product of the pulse voltage and the pulse current according to Eq. (14).

2. Decomposition of Organic Compounds and Nitric Oxide

The concentration profiles of toluene as a function of discharge power for different gas flow rates are shown in Fig. 5. The amount of the toluene decomposed corresponds to the difference between the initial (200 ppm) and the final concentration. In general, it is very clear that the decomposition of toluene increased with the increase in the discharge power. It has been reported that active oxygen species and long-lived ozone play an important role in the decomposition of toluene in a pulsed corona reactor [Yamamoto et al., 1993]. In addition, short-lived nitrogen species and direct electron impact are known to cleave the chemical bonds in the molecule [Ogata et al., 1999]. Therefore, the increase in the decomposition of toluene with the discharge power can be explained by the promotion of various reactive species production. At a flow rate of 0.083 L/s, the amounts of toluene decomposed at 5.5 W and 11 W were 60 and 100 ppm, respectively. When the flow rate was decreased to 0.033 L/s, the decomposition was largely enhanced, as shown in Fig. 5. In this case, the amounts of toluene decomposed were 115 and 152 ppm at 5.5 W and 11 W. Such enhancement in the decomposition is obviously due to the increase in the energy density with the decrease in the flow rate. As mentioned above, the energy density P_w/Q has widely been used as an important parameter capable of determining the decomposition efficiency.

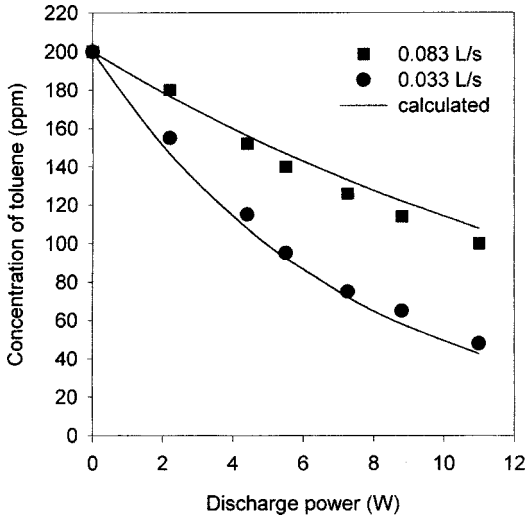

Fig. 5. Effect of the discharge power on the decomposition of toluene.

The effect of the discharge power on the decomposition of propylene is presented in Fig. 6. The trend of the decomposition of propylene was similar to that of toluene, but despite the increased flow

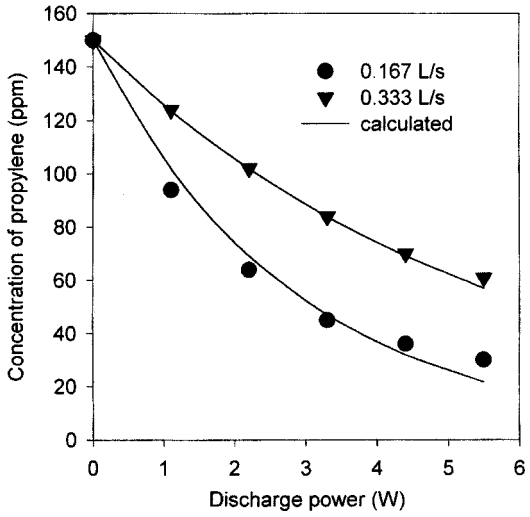

Fig. 6. Effect of the discharge power on the decomposition of propylene.

rate and the decreased discharge power, propylene was more easily decomposed than toluene. Previous studies have indicated that the decomposition efficiency of organic compound largely depends on its chemical structure. Since propylene has different molecular structure from toluene, the behavior such as reactivity with radicals and bond dissociation energy is necessarily different. According to the literature, the reactivity of propylene with O radical and ozone is known to be very high [Atkinson et al., 1992; Seinfeld, 1975]. The reaction rate constant between propylene and O radical is 6,810 ppm^{-1} min^{-1} at 298 K while that between toluene and O radical is only 107 ppm^{-1} min^{-1} at the same temperature [Seinfeld, 1975]. In addition, the benzene ring of toluene is so stabilized by resonance hybrid that the carbon-carbon bond cannot easily be broken [Hart et al., 2000].

Although the organic compounds can be decomposed by the pulsed corona discharge, it may generate some undesirable byproducts [Choi et al., 2000; Futamura et al., 1998, 1999; Mok et al., 2000a; Ogata et al., 1999]. As reported in many previous studies, most of the organic compounds decomposed in the plasma reactor are converted to CO_x ($CO+CO_2$), which is the desirable mode in this process [Futamura et al., 1999; Mok et al., 2000b; Ogata et al., 1999]. In this experimental condition, however, 2-5 ppm of formaldehyde and 4-9 ppm of ethane were detected at the reactor outlet. Among them, C_2H_6 is not regarded as a harmful volatile organic compound because of its low photochemical reactivity. On the other hand, formaldehyde has many harmful effects on the human body, and thus further study to minimize it is necessary.

Fig. 7 presents the concentration profiles of NO at the reactor outlet as a function of discharge power for different flow rates. As the discharge power increased, NO concentration decreased as a result of the reactions with the various active species. As expected, the amount of NO removed increased with the decrease in the flow rate due to the increase in the energy density. In the pulsed corona discharge process, radicals such as O, OH, HO_2, N and O_3 are involved in the removal of NO [Civitano, 1993; Lowke and Morrow, 1995; Mok et al., 1998; Sun et al., 1996]. Among them, OH and HO_2 can be produced only in the presence of H_2O. Note that this experiment was conducted in the absence of H_2O. Therefore, it is understood that the removal of NO in this experiment was mainly caused by O, N and O_3.

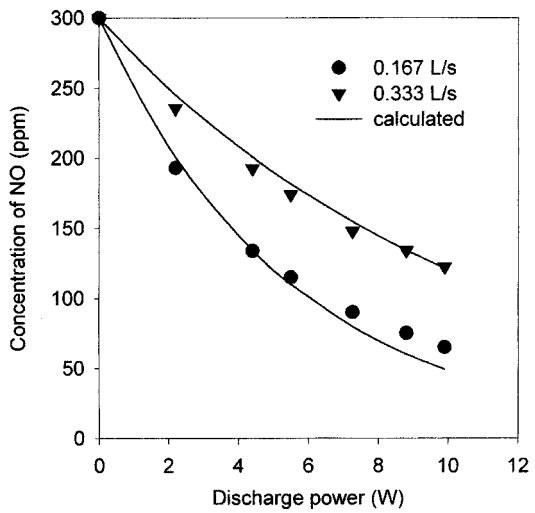

Fig. 7. Effect of the discharge power on the removal of nitric oxide.

Table 1. Explanation for the calculation of the apparent decomposition rate constant

Q (L/s)	ln C_{A0}/C_{AL}	P_W/Q (W s L^{-1})	k_d (L s^{-1} W^{-1})
0.333	0.190	3.3	5.77×10^{-2}
0.333	0.386	6.6	5.84×10^{-2}
0.333	0.580	9.9	5.86×10^{-2}
0.333	0.762	13.2	5.77×10^{-2}
0.333	0.900	16.5	5.45×10^{-2}
0.167	0.467	6.6	7.08×10^{-2}
0.167	0.852	13.2	6.45×10^{-2}
0.167	1.204	19.8	6.08×10^{-2}
0.333	1.427	26.4	5.41×10^{-2}
0.333	1.609	33.0	4.88×10^{-2}
	Average		5.86×10^{-2}

3. Decomposition Rate Constants

The overall reaction of the decomposition of the organic compounds and nitric oxide may be expressed as Eq. (5). So as to determine the apparent decomposition rate constant from the experimental data in Fig. 5 to Fig. 7, Eq. (12) derived above was applied to each point of the data. In the case of propylene, as an example, the calculation procedure of Eq. (12) can be summarized as Table 1. As shown in Table 1, the apparent decomposition rate constant of propylene was calculated to be 5.86×10^{-2} L s^{-1} W^{-1}. This value is the average of the results calculated at each point. For toluene, the apparent decomposition rate constant was found to be 4.68×10^{-3} L s^{-1} W^{-1} by the similar calculation. This is approximately 12.5 times smaller value than that of propylene. As mentioned above, toluene has low reactivity with active species and large bond dissociation energy. Likewise, the averaged rate constant of nitric oxide was found to be 3.06×10^{-2} L s^{-1} W^{-1}.

The concentration profiles calculated by using Eq. (10) and the

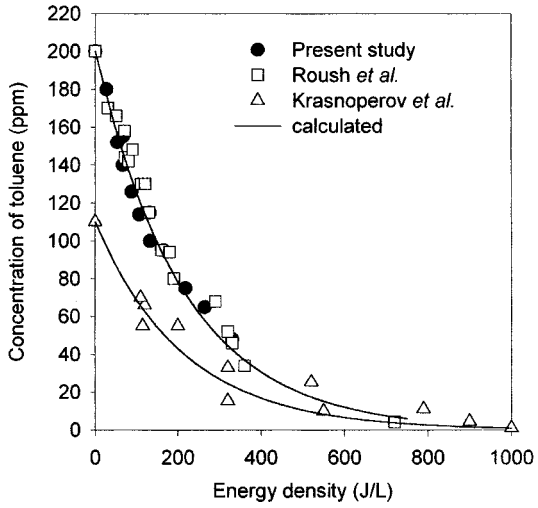

Fig. 8. Comparison between the experimental and calculated decomposition efficiency of toluene as a function of energy density.

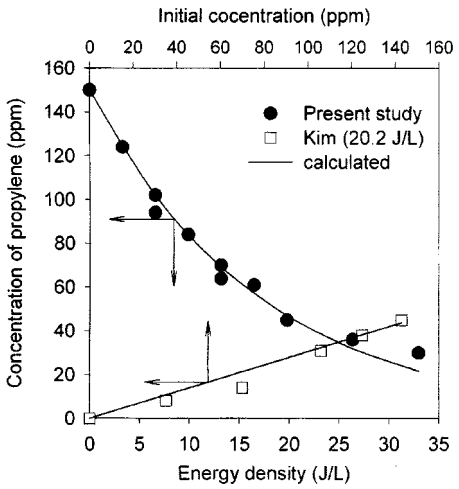

Fig. 9. Comparison between the experimental and calculated decomposition efficiency of propylene as a function of energy density.

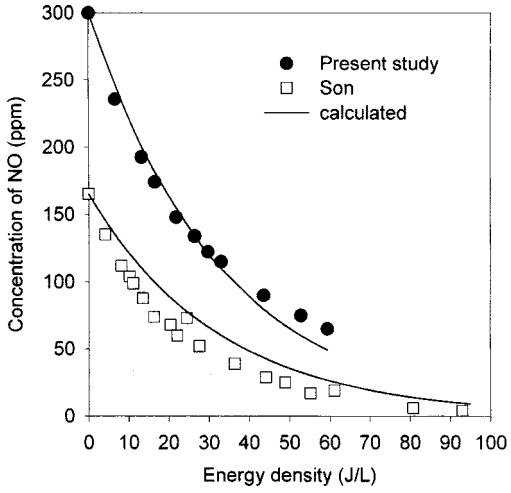

Fig. 10. Comparison between the experimental and calculated removal efficiency of nitric oxide as a function of energy density.

decomposition rate constants obtained above are also presented in Fig. 5 to Fig. 7. As can be seen, the calculation results track well all over the experimental data. Therefore, the decomposition rate constants determined are considered as appropriate. Fig. 8 to Fig. 10 compare the experimental data in the literature and the present study with the calculation results using the decomposition rate constants obtained above [Kim, 2000; Krasnoperov, 1997; Roush et al., 1996; Son, 1998]. Despite the different reactor geometry and the initial concentrations, the calculation results were able to predict the experimental data adequately.

Table 2 summarizes the apparent decomposition rate constants of several organic compounds calculated by applying Eq. (11) to the experimental data in the present study and in the literature [Krasnoperov, 1997; Penetrante et al., 1996; Roush et al., 1996; Snyder and Anderson, 1998; Song et al., 2000]. The organic compounds in Table 2 were classified into three groups by their chemical structure, namely, substituted alkane, alkene (or substituted alkene) and

Table 2. Apparent decomposition rate constants of organic compounds at 298 K

Pollutant	k_d (L s^{-1} W^{-1})	Classification
Carbon tetrachloride	2.48×10^{-3}	Substituted Alkane
Chlorobenzene	3.54×10^{-3}	Aromatic
Ethylene	2.73×10^{-2}	Alkene
Methanol	5.12×10^{-3}	Substituted alkane
o-xylene	6.22×10^{-3}	Aromatic
Propylene	5.86×10^{-2}	Alkene
Toluene	4.68×10^{-3}	Aromatic
Trichloroethylene	6.49×10^{-2}	Substituted Alkene

aromatics. As can be seen in Table 2, alkene and substituted alkene such as ethylene, propylene and trichloroethylene have very large decomposition rate constants while aromatic compounds and substituted alkanes such as carbon tetrachloride, methanol, toluene and ortho-xylene have small decomposition rate constants. As mentioned above, the decomposition rate of an organic compound is related to its chemical structure and reactivity with active species generated in a corona discharge. According to the literature, methane is known as the most stable organic compound, and the decomposition of it is very hard [Krasnoperov, 1997]. The small decomposition rate constants of carbon tetrachloride and methanol that are methane derivatives can be explained by the stability (low reactivity) due to their chemical structures. In case of aromatics, the carbon-carbon bond in benzene ring is very strong because of resonance hybrid, and they have low reactivity with active species as mentioned above [Hart et al., 2000; Seinfeld, 1975]. Therefore, it is very difficult to decompose the aromatic compounds in the corona reactor. It should be noted that all of the decomposition data in Table 2 were obtained by using air (80% N_2 and 20% O_2) as background gas and at room temperature. Under different background gas composition and temperature, the decomposition rate constant may be different.

CONCLUSIONS

The performance of the pulsed corona discharge process to decompose a gaseous pollutant such as toluene, propylene, and nitric oxide may best be characterized by the decomposition rate constant. To obtain the apparent decomposition rate constant, the performance equation of the corona reactor was derived with the assumption that the decomposition rate is directly proportional to the concentration and the discharge power. By using this model equation, the apparent decomposition rate constants of various gaseous organic compounds and nitric oxide were determined. The results show that the decomposition of alkene or substituted alkene is much easier than that of aromatics or substituted alkane. Experimental data were compared with the values predicted by model calculations. The model was able to predict well the experimental data in the present study and those in the literature.

ACKNOWLEDGMENT

This work was supported by Grant Number 2001-2-30900-001-2 from the Basic Research Program of the Korea Science & Eng-

ineering Foundation.

NOMENCLATURE

C_A : concentration of pollutant at any position in the reactor [parts per million, ppm]
C_{A0} : concentration of pollutant at reactor inlet [parts per million, ppm]
$C_{A,i}$: concentration of pollutant after treated by i-th pulsing [parts per million, ppm]
$C_{A,i-1}$: concentration of pollutant before treated by i-th pulsing [parts per million, ppm]
C_{AL} : concentration of pollutant at reactor outlet [parts per million, ppm]
D_e : axial dispersion coefficient [$m^2\ s^{-1}$]
E_P : energy delivered to the reactor per pulse [J]
f : pulse repetition rate (pulse frequency) [Hz]
I : pulse current [A]
k_d : apparent decomposition rate constant of pollutant [$L\ s^{-1}\ W^{-1}$]
P_W : average discharge power [W]
Q : total flow rate of feed gas stream [$L\ s^{-1}$]
Q_1 : flow rate of nitrogen [$L\ s^{-1}$]
Q_2 : flow rate of oxygen [$L\ s^{-1}$]
Q_3 : flow rate of nitrogen used for the saturation of toluene [$L\ s^{-1}$]
R_A : decomposition rate of pollutant [$ppm\ s^{-1}$]
t : pulse width [s]
u_0 : linear velocity of gas stream [$m\ s^{-1}$]
V : pulse voltage [V]
V_R : reactor volume [m^3]
z : any axial position in the corona reactor [m]

Greek Letters

τ : distance/linear velocity of gas stream, defined in Eq. (3) [s]
τ_P : pulse period, 1/f [s]
τ_L : total residence time of gas stream [s]

REFERENCES

Atkinson, R., Baulch, D. L., Cox, R. A., Hampson Jr., R. F., Kerr, J. A. and Troe, J., "Evaluated Kinetic and Photochemical Data for Atmospheric Chemistry: Supplement IV," *J. Phys. Chem. Ref. Data*, **21**, 1125 (1992).

Choi, Y. S., Song, Y. H., Kim, S. J. and Kim, B. U., "A Study on the Toluene Decomposition Using an Adsorptive Dielectric Discharge Plasma," *HWAHAK KONGHAK*, **38**, 423 (2000).

Civitano, L., "Industrial Application of Pulsed Corona Processing to Flue Gas," Non-Thermal Plasma Techniques for Pollution Control: Part B, Penetrante, B. M. and Schultheis, S. E., eds., Springer-Verlag, Berlin, 103 (1993).

Dinelli, G., Civitano, L. and Rea, M., "Industrial Experiments on Pulse Corona Simultaneous Removal of NO_x and SO_2 from Flue Gas," *IEEE Trans. Ind. Appl.*, **26**, 535 (1990).

Futamura, S., Zhang, A., Prieto, G. and Yamamoto, T., "Factors and Intermediates Governing Byproduct Distribution for Decomposition of Butane in Nonthermal Plasma," *IEEE Trans. Ind. Appl.*, **34**, 967 (1998).

Futamura, S., Zhang, A. and Yamamoto, T., "Mechanisms for Formation of Inorganic Byproducts in Plasma Chemical Processing of Hazardous Air Pollutants," *IEEE Trans. Ind. Appl.*, **35**, 760 (1999).

Hart, H., Craine, L. E. and Hart, D. J., "Organic Chemistry," Houghton Mifflin Company, Boston (2000).

Jeong, H. K., Kim, S. C., Han, C., Lee, H., Song, H. K. and Na, B. K., "Conversion of Methane to Higher Hydrocarbons in Pulsed DC Barrier Discharge at Atmospheric Pressure," *Korean J. Chem. Eng.*, **18**, 196 (2001).

Kim, J. H., "Simultaneous Removal of SO_2 and NO_x by Pulsed Corona Discharge Process," MS Thesis, Chem. Eng. Dept., Pohang Univ. of Science and Technol. (2000).

Krasnoperov, L. N., Krishtopa, L. G. and Bozzelli, J. W., "Study of Volatile Organic Compounds Destruction by Dielectric Barrier Corona Discharge," *J. Adv. Oxid. Technol.*, **2**, 248 (1997).

Lowke, J. J. and Morrow, R., "Theoretical Analysis of Removal of Oxides of Sulphur and Nitrogen in Pulsed Operation of Electrostatic Precipitators," *IEEE Trans. Plasma Sci.*, **23**, 661 (1995).

Mizuno, A., Shimizu, K., Chakrabarti, A., Dascalescu, L. and Furuta, S., "NO_x Removal Process Using Pulsed Discharge Plasma," *IEEE Trans. Ind. Appl.*, **31**, 957 (1995).

Mok, Y. S., Ham, S. W. and Nam, I., "Mathematical Analysis of Positive Pulsed Corona Discharge Process Employed for Removal of Nitrogen Oxides," *IEEE Tran. Plasma Sci.*, **26**, 1566 (1998).

Mok, Y. S., Kim, J. H., Ham, S. W. and Nam, I., "Removal of NO and Formation of Byproducts in a Positive Pulsed Corona Discharge Reactor," *Ind. Eng. Chem., Res.*, **39**, 3938 (2000a).

Mok, Y. S., Lee, H. W. and Hyun, Y. J., "Destruction of a Volatile Organic Compound Using Pulsed Plasma Discharge Process," *J. Environ. Res., Cheju National Univ.*, **8**, 81 (2000b).

Mok, Y. S., Lee, H. W., Hyun, Y. J., Ham, S. W., Kim, J. H. and Nam, I., "Removal of NO and SO_2 by Pulsed Corona Discharge Process," *Korean J. Chem. Eng.*, **18**, 308 (2001).

Oda, T., Kato, T., Takahashi, T. and Shimizu, K., "Nitric Oxide Decomposition in Air by Using Nonthermal Plasma Processing with Additives and Catalyst," *IEEE Trans. Ind. Appl.*, **34**, 268 (1998).

Ogata, A., Shintani, N., Mizuno, K., Kushiyama, S. and Yamamoto, T., "Decomposition of Benzene Using a Nonthermal Plasma Reactor Packed with Ferroelectric Pellets," *IEEE Trans. Ind. Appl.*, **35**, 753 (1999).

Penetrante, B. M., Hsiao, M. C., Bardsley, J. N., Merritt, B. T., Vogtlin, G. E., Wallman, P. H., Kuthi, A., Burkhart, C. P. and Bayless, J. R., "Comparison of Non-Thermal Plasma Techniques for Abatement of Volatile Organic Compounds and Nitrogen Oxides," Emerging Solutions to VOC & Air Toxics Control Conference, Clearwater Beach, Florida (1996).

Roush, R. A., Hutcherson, R. K., Ingram, M. W. and Grothaus, M. G., "Effects of Pulse Risetime and Pulse Width on the Destruction of Toluene and NO_x in a Coaxial Pulsed Corona Reactor," Proc. Twenty-Second International Power Modulator Symposium, Boca Raton, Florida, June 25-27, 78 (1996).

Seinfeld, J. H., "Air Pollution," McGraw Hill, New York (1975).

Shimizu, K., Kinoshita, K., Yanagihara, K., Rajanikanth, B. S., Katsura, S. and Mizuno, A., "Pulsed-Plasma Treatment of Polluted Gas Using Wet-/low-temperature Corona Reactors," *IEEE Trans. Ind. Appl.*,

33, 1373 (1997).

Snyder, H. R. and Anderson, G. K., "Effect of Air and Oxygen Content on the Dielectric Barrier Discharge Decomposition of Chlorobenzene," *IEEE Trans. Plasma Sci*., **26**, 1695 (1998).

Son, B. H., "Effect of Additive and Pulse Forming Capacitor for the Oxidation of NO in Pulsed Corona Discharge Process," MS Thesis, School of Environ. Eng., Pohang Univ. of Science and Technol. (1998).

Song, Y., Shin, D., Shin, W., Kim, K., Choi, Y., Choi, Y.-S., Lee, W. and Kim, S., "Characteristics of Non-Thermal Plasma Processes for Air Pollution Control," *J. Korean Soc. Atmospheric Envron.*, **16**, 247 (2000).

Sun, W., Pashaie, B. and Dhali, S. K., "Non-Thermal Plasma Remediation of SO_2/NO Using a Dielectric-Barrier Discharge," *J. Appl. Phys.*, **79**, 3438 (1996).

Tas, M. A., van Hardeveld, R. and van Veldhuizen, E. M., "Reactions of NO in a Positive Streamer Corona Plasma," *Plasma Chem. Plasma Proc*., **17**, 371 (1997).

Urashima, K., Chang, J. S., Park, J. Y., Lee, D. C., Chakrabarti, A. and Ito, T., "Reduction of NO_x from Natural Gas Combustion Flue Gases by Corona Discharge Radical Injection Techniques," *IEEE Trans. Ind. Appl*., **34**, 934 (1998).

van Veldhuizen, E. M., Zhou, L. M. and Rutgers, W. R., "Combined Effects of Pulsed Discharge Removal of NO, SO_2, and NH_3 from Flue Gas," *Plasma Chem. Plasma Proc.*, **18**, 91 (1998).

Yamamoto, T., Lawless, P. A., Owen, M. K. and Ensor, D. S., "Decomposition of Volatile Organic Compounds by a Packed-Bed Reactor and a Pulsed-Corona Plasma Reactors," Non-Thermal Plasma Techniques for Pollution Control: Part B, Springer-Verlag, Berlin, Germany, 223 (1993).